Rapid 3D Survey and GIS-Based Workflow for Heritage Risk Assessment. The Case Study of Mirandola, Italy

Nazarena Bruno [1] , Andrea Zerbi [1]

[1] University of Parma, dept. of Engineering and Architecture (DIA), Italy – (nazarena.bruno, andrea.zerbi)@unipr.it

Keywords: 3D survey, Spherical photogrammetry, GIS, Historical city centres, Risk assessment, Cultural Heritage.

Abstract

This paper investigates rapid survey methodologies for urban environments to support the compilation of the Italian *Carta del Rischio del Patrimonio Culturale* (Risk Map of Cultural Heritage, GIS developed by the Italian Ministry of Culture), with a focus on the documentation and assessment of *Building Fronts* in historic centres. The study addresses the need for acquisition strategies that balance accuracy requirements with constraints related to survey time and costs, while ensuring flexibility and long-term updatability. The proposed workflow was tested on a complete urban block in the historic centre of Mirandola (Modena, Italy), characterised by dense urban morphology, narrow streets, and ongoing post-seismic reconstruction. Data acquisition was based on spherical photogrammetry as the primary rapid survey technique, complemented by Google Street View panoramas to support diachronic analysis of façade transformations. A high-accuracy reference survey integrating Terrestrial Laser Scanning and Close-Range Photogrammetry was carried out on a limited portion of the block to validate the rapid survey results. Different ground control configurations were evaluated to assess the trade-off between acquisition speed and metric accuracy.
All survey products and diachronic imagery were integrated into a GIS-based information system structured according to the *Carta del Rischio* data model. The system enables immersive visualization of panoramic images, metric inspection of façade orthophotos, and structured data management, supporting monitoring, risk assessment, and conservation activities in historic urban contexts.

1. Introduction

This paper presents the initial results of an on-going research activity developed within the Italian PRIN 2022 project "*Vulnerability and risk of historical centres between depopulation, abandonment and extensive re-functionalization. Materials and tools for monitoring and managing historical buildings"*. The project aims to define analytical and evaluative methodologies for the built heritage of Italian historic centres through the use of advanced tools for data acquisition, organisation, and management. The main goal is to combine heritage protection and conservation requirements with the need for compatible and sustainable use over time. In this context, particular attention is given to the risks of loss affecting historic built environments, especially in relation to complex processes such as depopulation, abandonment, and extensive functional transformations.

A key methodological reference for this approach lies in risk-based assessment frameworks addressing the potential loss or degradation of historic urban centres (Masini et al., 2023; Pozzoni et al., 2024). Among these, the *Carta del Rischio del Patrimonio Culturale* (Risk Map of Cultural Heritage) represents a consolidated reference. Developed since the mid-1990s by the Central Institute for Restoration of the Italian Ministry of Culture, the *Carta del Rischio* was conceived to support heritage policies through a preventive strategy based on systematic conservation and maintenance actions (Cacace, 2019). It is structured as a Geographic Information System (GIS) that integrates data on environmental and anthropogenic hazards with information on the vulnerability of individual assets, providing a synthetic framework to support decision-making and intervention planning ("Carta del Rischio - MiC ICR - Cartografia"). Without addressing the full complexity of this multi-level information system, it is worth emphasising that the methodological framework of the *Carta del Rischio* is grounded in a knowledge-based process. This process combines the inventory of built heritage with the interpretation of architectural and constructional features and the assessment of conservation conditions, ultimately aimed at evaluating vulnerability. This approach reflects a well-established principle, also acknowledged at the regulatory level, according to which knowledge constitutes a fundamental prerequisite for any intervention on historic assets (Fiorani, 2019). One of the main challenges today concerns the organisation and operational use of the large amount of available information. In this respect, digital technologies and information systems play a central role, enabling the integration and management of heterogeneous datasets that were previously fragmented and poorly interoperable (Fiorani, 2019; Fiorani et al., 2022).

Within the PRIN project, the research focuses on the development of interoperable information management systems applicable to different geographical contexts across the national territory and capable of interfacing with the *Carta del Rischio.* These systems are conceived as GIS-based platforms dedicated to historic centres and designed as functional extensions of the *Carta del Rischio*. Their purpose is to support analysis, monitoring, and data updating at both urban and architectural scales (Fiorani et al., 2022). In this framework, the description and assessment of the existing built environment are articulated across multiple levels of analysis, ranging from the *Historical Centre* as a whole to *Urban Units*, *Urban Spaces*, *Building Units*, and *Building Fronts*, each associated with specific data models and survey forms.

The present paper addresses the preliminary phase of the research, which is devoted to data acquisition for the historic centres selected as pilot cases. The case study focuses on a complex urban block (Figure 1) located in the historic centre of

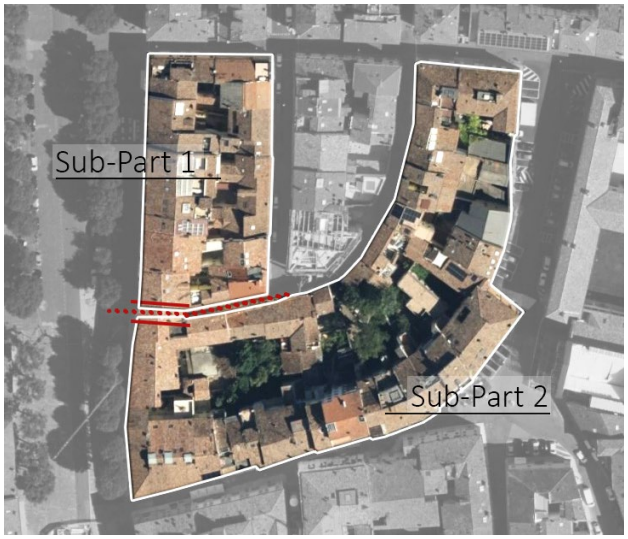

Figure 1. Overview of the selected urban block with its subdivision into two sub-parts; the narrowest internal street with a vaulted passage is indicated in red.

Mirandola (Modena, Italy), a city severely affected by the earthquake that struck the Emilia region in May 2012 and still undergoing extensive reconstruction and restoration processes. The relatively recent occurrence of the seismic event makes this context particularly significant, as it provides access to a substantial body of digital documentation produced both before and after the earthquake, which is essential for reconstructing and interpreting transformations in the historic built environment.

The study specifically focuses on rapid survey activities aimed at collecting the information required for compiling the *Building Front* forms defined within the *Carta del Rischio*. In parallel, a dedicated GIS was developed to ensure accessibility and usability by operators responsible for data compilation and updating. Survey activities were oriented towards the generation of a three-dimensional reconstruction of the selected urban block, conceived as a pilot area for testing fast and low-cost acquisition strategies capable of ensuring adequate geometric accuracy and visual documentation at the urban scale (Barazzetti and Roncoroni, 2021; Perfetti et al., 2023; Predari et al., 2019). In this perspective, the availability of heterogeneous digital data, such as time-referenced panoramic imagery and photographic documentation obtained from widely used digital platforms, offers the opportunity to conduct not only synchronic analyses of the current state of the built environment but also diachronic investigations based on the comparison of homogeneous datasets acquired at different times. The critical processing of these materials is therefore considered an integral component of an extended approach to rapid surveying, in which the collection and interpretation of historical digital data contribute to the construction of a comprehensive knowledge framework.

The overall objective of the research is to define a data acquisition and management workflow that balances accuracy requirements with constraints related to survey time and costs, while ensuring flexibility and long-term updatability. Within this framework, the developed information system integrates data derived from survey activities with historized digital sources, functioning both as an operational support tool for compiling the *Carta del Rischio* forms and, more broadly, as a knowledge management environment supporting the conservation and protection of historic built heritage.

2. Materials and methods

Data acquisition was designed to document *Building Fronts* at the scale of an entire urban block, while ensuring a methodology that could be rapidly deployed, replicated over time, and easily extended to larger portions or transferred to other historic urban context. In this framework, the main objectives of the survey were to:

- collect reliable and sufficiently detailed data for the documentation of the building façades, suitable for remote consultation and analysis;
- test rapid and scalable survey methodologies capable of guaranteeing adequate levels of geometric accuracy and readability of both the current condition of the façades and their transformations;
- enable a diachronic reading of transformations affecting the built environment.

The selected case study is a U-shaped urban block located within a densely built urban fabric, which covers an area of approximately 9563 m² and includes a total linear extension of building façades of about 566 m. This distinctive shape encloses a second inner block, creating a system of narrow internal streets that separate the two blocks. These internal streets are also only partially accessible, due to the presence of scaffolding and ongoing restoration works. The U-shaped block itself can be subdivided into two sub-portions (Sub-part 1 and Sub-part 2), separated by a very narrow street (3 m) that is partially covered by a vaulted passage, where the roadway runs beneath the buildings, further complicating data acquisition (Figure 1).

Spherical photogrammetry was identified as the primary rapid survey technique due to its ability to capture full 360° imagery from a single acquisition position, significantly reducing fieldwork time while providing dense visual coverage of the urban environment (Fangi et al., 2018; Rezaei et al., 2024). It was preferred over SLAM-based mobile mapping solutions because it provides high-quality and directly navigable images (essential for visual inspections) and ensures significantly lower costs.

Spherical photogrammetry allows the generation of two complementary types of outputs: traditional photogrammetric products, such as three-dimensional models and orthophotos, and navigable panoramic images that can be directly explored without additional processing. These panoramas are of the same type as Google Street View (GSV) imagery, facilitating seamless integration and direct comparison with historical datasets at no additional acquisition cost. By leveraging these two types of outputs, the rapid survey workflow was designed to achieve two main objectives: (i) acquire geolocated spherical images suitable for GIS integration and remote inspection of building façades; and (ii) derive metric information, including Digital Surface Models (DSMs) and orthophotos, through standard photogrammetric processing.

To ensure metric reliability and enable accuracy assessment, all survey activities were supported by a topographic control network established using total station and GNSS measurements. In addition, Sub-Part 1 of the block was also surveyed using a traditional, high-accuracy approach based on the integrated use of Terrestrial Laser Scanning (TLS) and Close-Range Photogrammetry (CRP), which served as reference data for validating DSMs and orthophotos obtained from the rapid survey.

2.1 Reference high-accuracy survey: topographic control network, CRP and TLS

The topographic control network was established around the entire urban block and consisted of 13 survey stations, from which 67 architectural points on the façades were measured to be used both as Ground Control Points (GCPs) and Check Points (CPs). The selection of architectural features, although not optimal in terms of point definition and measurement accuracy, was dictated by the impossibility of installing artificial targets on the façades. The network was subsequently georeferenced by surveying the positions of seven stations using GNSS observations (Figure 2.a). Particular attention was taken to select station points corresponding to easily recognizable features at the street-level, so that they could be reliably recognised and collimated in the acquired imagery. Due to the dense urban environment, the acquisition of reliable GNSS positions was challenging, mainly because of limited satellite visibility and multipath effects.

The laser scanning survey (only in Sub-part 1) was carried out using a Leica RTC360 terrestrial laser scanner, acquiring a total of 43 scans (Figure 2.b). The same portion of the urban block was also surveyed using Close-Range Photogrammetry, employing a full-frame Nikon D3x DSLR camera (6048 × 4032 pixels resolution, 6 µm pixel size) equipped with a 35 mm Nikkor lens. A total of 489 images were acquired (Figure 2.b). All fieldwork activities, including the establishment of the topographic control network, required a full working day for two operators.

An integrated processing of TLS and photogrammetric data was performed (Bruno et al., 2022). The TLS scans were first pre-registered using a cloud-to-cloud approach in Leica Cyclone Register 360 and subsequently imported into Agisoft Metashape, which allows the integration of TLS data. Given the high internal consistency achieved during the TLS pre-registration, the relative orientation of the laser scans was preserved during import and only their absolute georeferencing was refined using GCPs derived from the topographic survey. In this configuration, the TLS data were then used as a geometric reference for the orientation of the CRP images. As the laser scans were imported together with their associated panoramic images, interpreted as cube maps, they could be jointly processed with the photogrammetric images using a standard image-matching approach. The orientation parameters of the cube maps were kept fixed and used as reference, while the exterior orientation parameters of the CRP images were estimated during the Bundle Block Adjustment (BBA) based on tie points shared between the two datasets. This procedure preserves the original TLS registration and allows the photogrammetric images to be oriented without the need for additional GCPs.

The integrated processing resulted in a Root Mean Square Error (RMSE) of 2.1 cm on the CPs. The processing pipeline produced a high-resolution DSM (Figure 3.left), which was adopted as the geometric reference for the validation of the rapid survey results and for the generation of façade orthophotos at a spatial resolution of 2 mm/pixel (Figure 3.right).

2.2 Rapid survey using spherical photogrammetry

Over the entire urban block, the survey was conducted using an INSTA360 Pro2 spherical camera. The device is equipped with six sensors, each acquiring fisheye images with a resolution of 4000 × 3000 pixels and a field of view of approximately 200° (focal length 1.88 mm, aperture F2.4). The camera records raw fisheye images and can also generate stitched equirectangular panoramas in real time, with a resolution of 7680 × 3840 pixels. An integrated GNSS antenna records positional metadata – latitude, longitude, and altitude – for each acquisition position.

The camera was mounted on a backpack, and the operator walked along the streets of the historical centre, capturing 360° imagery at regular intervals of 2 seconds, resulting in an average base length of approximately 1.35 m. Due to the narrow and elongated configuration of the streets, and in order to strengthen the geometric rigidity of the photogrammetric block and reduce potential systematic rotations, two acquisition strips were collected for each street, laterally offset across the street

Figure 2. a. Topographic network and GNSS Ground Control Points; b. Integrated survey from TLS (light-blue) and CRP (blue).

Figure 3. DSM (left) and orthophoto (right) of the west urban front obtained from integrated processing of TLS and CRP data.

Figure 4. Spherical photogrammetry image block around the entire urban block. Image acquisition positions are highlighted in red.

width. Overall, 7134 images were acquired from 1189 shooting positions, with an average Ground Sampling Distance (GSD) of 2.6 mm/pixel. The total acquisition time was limited to approximately 45 minutes (Figure 4).

The photogrammetric processing was performed in Agisoft Metashape directly on the raw fisheye images acquired by the individual sensors. As highlighted in previous studies (Bruno et al., 2024; Perfetti et al., 2024) the physical configuration of spherical cameras – characterized by non-coincident projection centres with measurable offsets between sensors – makes the assumption of a single centre of projection for stitched panoramas geometrically inconsistent and prone to significant distortions. For this reason, the processing was carried out on the individual fisheye images rather than on the stitched equirectangular panoramas, following the methodology proposed in (Perfetti et al., 2024): to account for the fixed spatial relationships between the six sensors, the image sets acquired at each shooting position were modelled as a multi-camera system. A rigid constraint was imposed by defining fixed relative position and orientation parameters between each sensor and a designated master sensor. Within this framework, only the Exterior Orientation parameters of the master sensor were estimated during the BBA, while the orientations of the remaining sensors were derived from invariant Relative Orientation parameters. This strategy improves internal geometric consistency and reduces the degrees of freedom of the adjustment.

For consistency with the detailed CRP+TLS survey, two separate processing workflows were carried out: one covering the entire urban block and one limited to Sub-part 1. Four different ground constraint configurations, with decreasing levels of control, were evaluated to investigate the extent to which survey speed can be increased while maintaining acceptable accuracy:

A. **High constraint**: 23 GCPs (10 within Sub-part 1) derived from the topographic survey;
B. **Medium constraint**: 7 GCPs (3 within Sub-part 1) corresponding to ground points surveyed with GNSS;
C. **Low constraint**: 4 GCPs obtained from available regional cartographic datasets, with the camera centre positions recorded by the camera's onboard GNSS sensor used to initialise the image block orientation;
D. **No ground constraint**: 0 GCPs, relying on direct georeferencing based on the camera's onboard GNSS sensor, with the recorded camera centre positions used to directly orient the image block.

While a topographic control network (Scenario A) ensures the most robust and accurate results, it is often impractical in large urban areas due to the time and effort required for both data acquisition and processing. The medium-constraint configuration (Scenario B), based on GNSS-surveyed ground control points, represents a faster and more scalable alternative. This is facilitated by the nature of spherical imagery, which systematically captures ground-level elements and therefore simplifies the identification of natural control points. However, in dense urban environment, GNSS surveying cannot always be carried out under optimal conditions and may introduce non-negligible uncertainties. Scenario C was designed to avoid in situ ground control measurements, by relying on official institutional cartographic datasets. In this configuration, the GCPs were identified planimetrically on recognisable features visible in regional orthophotos, while elevation values were extracted from the regional Digital Terrain Model (DTM). The camera centre positions recorded by the onboard GNSS sensor were incorporated into the stochastic model of the BBA with a low weight (σ = 10 m) and used solely to initialise the image block orientation. Finally, direct georeferencing without any GCP (Scenario D) was tested by exploiting the GNSS data recorded by the spherical camera, in order to evaluate its suitability for a preliminary – albeit approximate – positioning of the camera trajectory. In this case, camera centre positions were included in the BBA with a moderate weight (σ = 1 m), so as not to excessively constrain the relative orientation between images and to favour the internal geometric coherence of the image block. Given the characteristics of the embedded GNSS sensor and the challenging acquisition conditions, low absolute positioning accuracy was expected for this configuration. Table 1 summarizes the acquisition parameters and processing pipelines adopted in different scenarios. In all cases, accuracy was assessed using the same set of CPs: 44 CPs for the entire urban block and 17 CPs for Sub-part 1.

Site	# Img.	# Shooting points	Constraint scenario	GCP	CP
1. Sub-part 1	2784	464	**A**	10	17
			B	3	17
			C	4	17
			D	0	17
2. Urban block	7134	1189	**A**	23	44
			B	7	44
			C	4	44
			D	0	44

Table 1. Summary of data acquisition and processing pipelines

In addition, the raw fisheye images were stitched using InstaStitcher software to produce equirectangular panoramas intended exclusively for visualization and navigation within a GIS environment. For their georeferencing, the mean coordinates of the camera centres of projection estimated during the photogrammetric processing were used.

2.3 Google Street View imagery

To enable a multitemporal analysis of the transformations affecting the urban block, spherical imagery provided by Google Street View was integrated into the study. GSV offers a time-series of panoramic images covering extended periods, which can be exploited for diachronic observations of the built environment. Although GSV imagery was not originally

acquired for metric purposes and presents intrinsic limitations in terms of geometric accuracy, its spatial continuity and temporal availability make it suitable for qualitative, large-scale monitoring applications.

Google provides downloadable equirectangular panoramas (up to 13312 × 6656 pixels), together with metadata including geographic coordinates (longitude, latitude, elevation), camera orientation, and acquisition date. In addition, depth maps are associated with each panorama, from which approximate three-dimensional information can be derived. All GSV datasets available for the study area were identified and downloaded, covering the years 2010, 2017, 2018, 2019, and 2025. This temporal span is particularly significant for the selected case study, as it includes imagery acquired prior to the 2012 Emilia earthquake as well as several post-event epochs, enabling the observation of both damage evolution and the progressive development of restoration and reconstruction works. Figure 5 shows an example of façade changes observed across different acquisition dates for a portion of the urban block.

The selected GSV panoramas were organised according to their acquisition date and shooting position and integrated into a GIS environment as geolocated point layers and visualised through immersive panorama viewers. Although GSV imagery can, in principle, be processed photogrammetrically, this option was deliberately excluded. As discussed in (Bruno and Roncella, 2019), GSV imagery can be used for three-dimensional reconstruction only when high metric accuracy is not required, as the resulting models and digital surface representations are generally affected by significant noise. Since the present study requires reliable metric documentation at the scale of façade, this approach was deliberately avoided. Consequently, the GSV images were not oriented or modelled, but used exclusively for immersive visualisation, remote inspection, and diachronic interpretation of façade transformations.

Figure 5. Multi-temporal Google Street View panoramas: pre-earthquake scenario (2010, top) and post-seismic restoration phase (2018, bottom).

3. Results

3.1 Rapid survey accuracy assessment

The validation of the rapid spherical photogrammetric survey was carried out by analysing three complementary aspects, systematically evaluated for each of the adopted control scenarios:

- Differences in the estimated Camera Centres of Projection (CCP) positions;
- Residuals on CPs, obtained from each processing pipeline;
- Differences between the DSMs generated from the spherical photogrammetry workflows and the DSM derived from the integrated CRP–TLS survey, assumed as ground truth.

3.1.1 Camera Centres of Projection analysis

The analysis of camera centre positions primarily aims to assess the reliability of spherical image geolocation for rapid visual inspection and GIS integration purposes. Specifically, the analysis investigates whether the positions recorded by the camera's embedded GNSS sensor are sufficiently accurate to allow the use of panoramic imagery without performing photogrammetric orientation, in cases where metric reconstruction of the urban block is not required. In addition, the effect of different ground control configurations on the estimation of CCP position is evaluated, in order to quantify how varying levels of control influence the final estimates. For this analysis, the CCP coordinates computed in the high-constraint solutions (Scenario A) were assumed as reference, under the reasonable assumption that the use of a dense topographic control network provides the most accurate estimates. This assumption is also confirmed by the low CP residuals discussed in Section 3.1.2 (Table 3). The CCP coordinates obtained under all other constraint configurations (Scenarios B, C, and D) were then compared against this reference solution. In addition, for the processing of the entire urban block, the raw GNSS coordinates recorded by the camera's embedded sensor were also compared with the reference solution, in order to assess their standalone reliability. Table 2 reports the RMSE values of the resulting differences, together with the maximum observed discrepancies.

Pipeline code	Centres of Projections RMSE [m]				Max [m]
	X	Y	Z	XYZ	
1.B – 1.A	0.255	0.205	0.056	0.332	0.746
1.C – 1.A	0.448	0.251	0.339	0.615	1.408
1.D – 1.A	1.374	1.974	1.126	2.656	3.730
Raw GPS – 2.A	5.764	5.198	7.982	11.133	40.14
2.B – 2.A	0.118	0.165	0.054	0.210	0.557
2.C – 2.A	0.583	0.381	0.133	0.709	1.243
2.D – 2.A	1.102	1.454	1.666	2.470	3.881

Table 2. RMSE and maximum differences of CCP positions.

The results clearly show that the raw GPS positions recorded by the spherical camera are highly inaccurate and unstable, with discrepancies reaching up to approximately 40 m. The largest inconsistencies are observed in the vertical component: while the actual elevation variation within the urban block is about 2 m, the camera GPS reports a vertical range of up to 46 m.

When the image block is oriented, even without external GCPs (Scenario D), discrepancies in the estimated CCP are significantly reduced, reaching values of ca. 2.5 m. Although this level of accuracy is insufficient for rigorous metric

reconstruction, it can be considered adequate for reliably positioning panoramic images in front of façades for visual inspection and qualitative analysis. With the introduction of a limited number of GCPs derived from official cartographic datasets (Scenario C), the CCP residuals decrease to about 60–70 cm, depending on whether the analysis is performed on Sub-part 1 or on the entire urban block. When GPS-surveyed GCPs are used (Scenario B), the discrepancies are further reduced to approximately 0.2–0.3 m.

3.1.2 CP residuals analysis

The accuracy of the final object reconstruction was evaluated by analysing the residuals on independent Check Points. Table 3 reports the Root Mean Square Error (RMSE) of the CP residuals for the different processing pipelines.

Pipeline code	CP RMSE [m]			
	X	Y	Z	XYZ
1.A	0.048	0.036	0.008	0.061
1.B	0.320	0.257	0.060	0.414
1.C	0.561	0.282	0.362	0.724
1.D	1.097	1.896	0.905	2.370
2.A	0.034	0.034	0.014	0.051
2.B	0.153	0.171	0.056	0.237
2.C	0.584	0.370	0.145	0.707
2.D	1.057	1.461	1.558	2.383

Table 3. RMSE of CP residuals.

As expected, the high-constraint solutions yield the most accurate results, with CP RMSE values of approximately 5 cm for the processing of the entire urban block (2.A) and about 6 cm for Sub-part 1 (1.A). At first glance, the slightly higher RMSE observed for the smaller area may appear counterintuitive. However, this difference is largely attributable to the different number of CPs used in the statistical evaluation (44 for the entire block and 17 for Sub-part 1). When the RMSE of pipeline 2.A is recalculated considering only the same 17 CPs used for Sub-part, the value increases to 6.3 cm. This confirms that, at a local scale, the smaller block is slightly more stable and accurately reconstructed, and that the apparent discrepancy is mainly a statistical effect.

For the medium-constraint scenario (Scenario B), a different behaviour is observed: irrespective of the number of CPs considered, the solution performs more reliably over the entire urban block (2.B) than over the smaller Sub-part (1.B). This outcome is primarily related to the number and spatial distribution of the GPS-derived GCPs. In dense urban environments, GNSS measurements can only be acquired in relatively open areas, such as squares or wider street sections. While seven GPS points could be measured and well distributed across the entire block, only three such points were available for Sub-part, all located along its northern and western edges. This uneven and limited control does not provide an optimal geometric constraint for the smaller area. Conversely, at the scale of the entire block, the higher number and better spatial distribution of GPS points result in a more robust network geometry and improved block stability. In absolute terms, the errors are mainly concentrated in the horizontal component and the largest residuals are observed in the CP along the narrowest and least accessible streets.

The low-constraint solutions (Scenario C) exhibit error magnitudes comparable to those previously observed for the residuals in CCP positioning, with RMSE values of approximately 70 cm. While such accuracy can be considered sufficient for the correct spatial placement of panoramic images intended for visual inspection, it is inadequate to ensure a metrically reliable reconstruction of building façades. Consequently, this configuration cannot be considered suitable for metric purposes. The same problem is even more evident in Scenario D, where planimetric (XY) errors reach approximately 1.8 m for the entire urban block and 2.2 m for Sub-part 1, with corresponding vertical errors of about 1.5 m and 0.9 m, respectively.

3.1.3 DSM comparison

The comparison between Digital Surface Models (DSMs) was performed exclusively on the Sub-Part 1, as this is the only area for which high-resolution reference data from the integrated TLS–CRP survey was available. For each processing pipeline, DSMs were generated only for this subset of the urban block. Scenarios C and D were excluded from the comparison due to the significant inconsistencies observed between the resulting models and the actual geometry, as already evidenced by the large residuals on the CPs. As expected, the DSMs derived from spherical photogrammetry appear visually noisier and less detailed than those obtained from the integrated TLS–CRP survey, with discrepancies that are particularly evident in the upper portions of the façades.

Although all DSMs were already referred to the same reference system, an Iterative Closest Point (ICP) algorithm was applied to optimise the registration and minimise residual systematic errors. The comparisons were performed in CloudCompare by evaluating signed distances between the models. Since the final objective is the analysis of individual façades, the comparisons were carried out separately for the north, south, east, and west fronts, allowing a façade-specific optimisation of the co-registration. Table 4 reports the RMSE of the DSM differences.

The results indicate that, with a sufficient number of GCPs, the differences between the spherical photogrammetry DSMs and the TLS–CRP reference are on the order of a few centimetres. These discrepancies are mainly attributable to surface noise in the mesh, which is more pronounced in the upper parts of the façades (Figure 6). With medium constraint, the north and west façades still show limited differences, whereas larger discrepancies are observed on the south and east façades. In these areas, the façades appear elongated towards the south-east corner, resulting in systematic differences of several

Pipeline code	DSM RMSE [cm]			
	North F.	South F.	East F.	West F.
1.A	3.05	4.01	3.48	3.08
1.B	7.94	13.47	12.92	6.25
2.A	2.73	3.74	3.63	3.77
2.B	2.98	11.50	12.42	5.56

Table 4. DSM RMSE values for individual front with respect to integrated TLS–CRP survey.

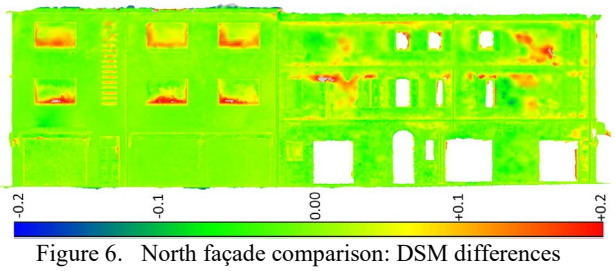

Figure 6. North façade comparison: DSM differences between INSTA360 spherical photogrammetry (pipeline 2.A) and TLS–CRP reference (−0.2 m blue, +0.2 m red).

Figure 7. INSTA360 North façade orthophoto (pipeline 2.A).

centimetres. This effect indicates a scale deformation along the acquisition trajectory direction and is consistent with the lower degree of geometric constraint in this portion of the block, which is also the least accessible area and the most weakly supported by GPS-derived control points.

Despite the observed differences in the DSMs, the orthophotos generated from the spherical photogrammetry models (Figure 7) remain suitable for documentation purposes. Areas exhibiting the largest DSM deviations generally correspond to surfaces with low texture (e.g., extended plastered façades) or to the upper portions of the buildings; however, these effects are largely mitigated in the orthophotos. The resulting orthophotos achieve a spatial resolution of 5 mm/pixel, which is sufficient for identifying the elements of interest required for the compilation of the *Carta del Rischio* forms and to support qualitative assessments of façade conditions.

3.2 Geographic information system implementation

The GIS was developed to integrate, organise, and operationally exploit the datasets generated through the survey activities described above. Its primary purpose is to provide a coherent environment for visualising and querying the acquired data and to support the compilation of the *Carta del Rischio* forms, which is currently still performed manually. In this framework, the GIS acts both as a structured repository of heterogeneous information and as a visualisation and analysis tool to assist operators during data interpretation and data entry. The system was entirely implemented using the open-source solution QGIS. All datasets derived from the integrated CRP–TLS survey, the spherical photogrammetric acquisitions, and the Google Street View imagery were imported and structured within the GIS environment. The information structure was explicitly designed to mirror the data model of the *Carta del Rischio*, in order to guarantee interoperability and future integration with ministerial databases. In particular, the implementation focused on the *Building Unit* and *Building Front* levels.

The GIS architecture integrates both open-access cartographic datasets (regional geodatabases, cadastral layers, orthophotos, Digital Terrain Models, and thematic vector layers) and the newly acquired survey data. The spherical images discussed in Sections 2.2 and 2.3 were stored as georeferenced point features and linked to embedded spherical viewers, allowing immersive and interactive visualisation directly within the GIS environment (Figure 8). This enables remote inspection of façade conditions and contextual analysis using the same type of panoramic imagery across different acquisition epochs, supporting diachronic interpretation without the need for external viewing tools. Façade orthophotos were explicitly associated with the corresponding *Building Front* entities. When queried, each orthophoto is displayed through a dedicated custom interface developed within QGIS. The orthophoto is opened in a separate floating map canvas and assigned to a local façade-based reference system, aligned with the plane of the building front. This configuration allows metric measurements – such as distances, crack extents, or opening widths – to be performed directly on the orthophoto, preserving consistency with the original survey geometry. The interface was implemented through a lightweight Python script based on the QGIS API, fully integrated into the GIS environment.

All GIS layers were enriched with attribute fields corresponding to the information required by the *Carta del Rischio* forms. In this way, the system functions both as a structured knowledge repository and as an operational support tool for data compilation and updating. Finally, data portability and field operability were addressed through the use of QField, an open-source mobile application that allows QGIS projects to be synchronised on portable devices. This enables operators to

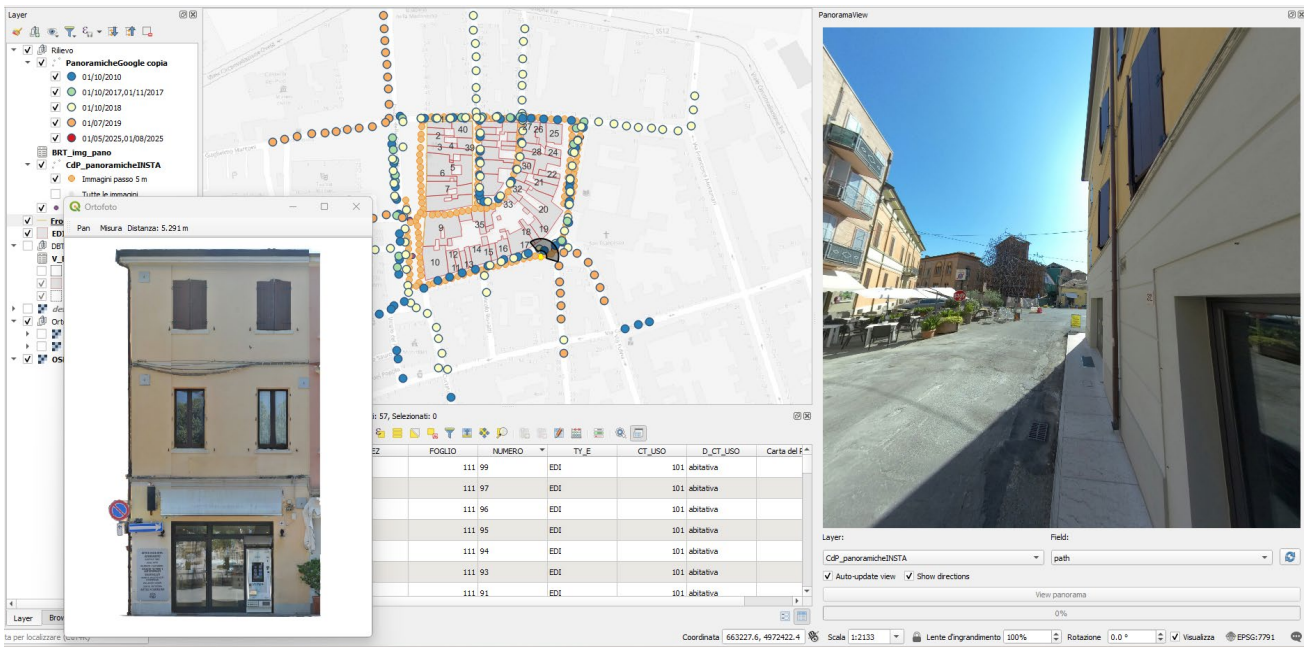

Figure 8. Example of the GIS interface allowing access to both orthophoto and panoramic image visualization.

access the same datasets in the field, visualise survey products, and directly update attribute information during inspections, ensuring continuity between in-office analysis and on-site data collection.

4. Conclusions

This paper investigated rapid survey technologies for the documentation of historic urban centres, with specific reference to the needs of the Italian *Carta del Rischio del Patrimonio Culturale*. The research addressed the challenge of balancing geometric accuracy with constraints related to acquisition time, operational costs, and long-term updatability.

The results demonstrate that spherical photogrammetry represents a highly effective solution for rapid urban surveys. The possibility of acquiring complete 360° imagery from a single acquisition position significantly reduces fieldwork time, while ensuring continuous visual coverage of façades. This approach enables the simultaneous production of metric outputs – DSMs and orthophotos – and immersive panoramic images that can be directly explored. The latter, being fully compatible with Google Street View imagery, allow seamless integration with these open datasets and support diachronic analyses of façade transformations without additional acquisition efforts.

From a metric perspective, the experiments confirm that the embedded GNSS sensor of spherical cameras is not sufficient for accurate georeferencing in dense urban environment. Nevertheless, GNSS observations can be effectively exploited to initialise BBA when the primary objective is panorama positioning for visual inspection. When metric products are required, a limited number of GNSS-surveyed GCPs is sufficient to achieve accuracies of a few centimetres. Official regional cartographic datasets can be used to densify GCPs in areas where GNSS measurements are difficult or partially obstructed, maintaining low operational effort.

All survey outputs were integrated within a GIS-based environment, structured to support immersive visualisation, metric inspection of façade orthophotos, and structured data management in line with the *Carta del Rischio* data model. By enabling remote inspection, multi-temporal comparison, and direct data updating, the GIS acts as both an operational tool for form compilation and a broader knowledge management environment for monitoring and risk assessment purposes.

Future developments may focus on automation of façade feature recognition, extraction of vulnerability indicators, and definition of robust procedures for temporal updating, with the aim of supporting continuous and long-term monitoring strategies.

Acknowledgements

Research funded under the Italian PRIN: Progetti di Ricerca di Rilevante Interesse Nazionale – 2022 project "Vulnerability and risk of historical centers between depopulation, abandonment and extensive re-functionalization. Materials and tools for monitoring and managing of historical buildings". Project code: 2022FABEHA, CUP: D53C24004840006. Principal investigator: Donatella Fiorani.

References

Barazzetti, L., Roncoroni, F., 2021. Generation of a multi-scale historic BIM-GIS with digital recording tools and geospatial information. *Heritage* 4, 3331–3348.

Bruno, N., Mikolajewska, S., Roncella, R., Zerbi, A., 2022. Integrated Processing of Photogrammetric and Laser Scanning Data for Frescoes Restoration. *Int. Arch. Photogramm. Remote Sens. Spat. Inf. Sci.* 46, 105–112.

Bruno, N., Perfetti, L., Fassi, F., Roncella, R., 2024. Photogrammetric survey of narrow spaces in cultural heritage: comparison of two multi-camera approaches. I*nt. Arch. Photogramm. Remote Sens. Spat. Inf. Sci*. XLVIII-2/W, 87–94.

Bruno, N., Roncella, R., 2019. Accuracy assessment of 3d models generated from Google Street View imagery. *Int. Arch. Photogramm. Remote Sens. Spat. Inf. Sci.* XLII-2/W9, 181–188.

Cacace, C., 2019. La carta del rischio per il patrimonio culturale, in: Fiorani, D. (Ed.), Il Futuro Dei Centri Storici. Digitalizzazione e Strategia Conservativa. Edizioni Quasar, Roma.

Carta del Rischio - MiC ICR - Cartografia. URL http://www.cartadelrischio.beniculturali.it/webgis/ (accessed 1.19.26).

Fangi, G., Pierdicca, R., Sturari, M., Malinverni, E.S., 2018. Improving spherical photogrammetry using 360°OMNI-Cameras: Use cases and new applications. *Int. Arch. Photogramm. Remote Sens. Spat. Inf. Sci.*, XLII-2, 331–337.

Fiorani, D., 2019. Introduzione, in: Fiorani, D. (Ed.), Il Futuro Dei Centri Storici. Digitalizzazione e Strategia Conservativa. Edizioni Quasar, Roma.

Fiorani, D., Acierno, M., Donatelli, A., Cutarelli, S., Martello, A., 2022. Centri storici, digitalizzazione e restauro Applicazioni e prime normative della Carta del Rischio. Sapienza Università Editrice, Roma.

Masini, P., Porta, M., Barazzetti, L., Oteri, A.M., 2023. Data organization using gis for a more conscious conservation approach for abandoned sites. *Int. Arch. Photogramm. Remote Sens. Spat. Inf. Sci.,* XLVIII-M-2, 1035–1042.

Perfetti, L., Bruno, N., Roncella, R., 2024. Multi-Camera Rig and Spherical Camera Assessment for Indoor Surveys in Complex Spaces. *Remote Sens.* 16, 4505.

Perfetti, L., Vassena, G.P.M., Fassi, F., 2023. Preliminary survey of historic buildings with wearable mobile mapping systems and uav photogrammetry. *Int. Arch. Photogramm. Remote Sens. Spat. Inf. Sci.*, XLVIII-M-2, 1217–1223.

Pozzoni, L., Barazzetti, L., Cuca, B., Oteri, A.M., 2024. An integrated hbim-gis digital environment for heritage preservation and enhancement in the inner italian territory. *Int. Arch. Photogramm. Remote Sens. Spat. Inf. Sci.*, XLVIII-2-W4, 357–364.

Predari, G., Bartolomei, C., Morganti, C., Mochi, G., Gulli, R., 2019. Expeditious methods of urban survey for seismic vulnerability assessments. *Int. Arch. Photogramm. Remote Sens. Spat. Inf. Sci.*, XLII-2-W17, 271–278.

Rezaei, S., Maier, A., Arefi, H., 2024. Quality Analysis of 3D Point Cloud Using Low-Cost Spherical Camera for Underpass Mapping. *Sensors* 24, 3534.